Arab J Sci Eng (2016) 41:5093–5109
DOI 10.1007/s13369-016-2211-6

RESEARCH ARTICLE - COMPUTER ENGINEERING AND COMPUTER SCIENCE

A Flexible and Cost-Effective Heterogeneous Network Deployment Scheme for Beyond 4G

M. Arthi[1] · **P. Arulmozhivarman**[2]

Received: 31 December 2015 / Accepted: 11 May 2016 / Published online: 30 May 2016

Abstract The network capacity has to be maximized to support the ever-increasing data traffic demand. One of the potential outcomes to enhance the network capacity is to enhance the spectral efficiency per unit area by expanding the serving node densities. This is unreasonable on account of present Macro evolved node B (eNB) for which site acquisition is expensive. The idea of heterogeneous network (HetNet) and multi-hop relay (MHR) are extremely prominent in long-term evolution (LTE) standard, where small cells are deployed along with Macro cell. Small cells are more suitable solution for the coverage and traffic issues experienced by Macro cell users. Unfortunately, HetNet deployment is not specified in any of the standards. The network operators have been managing tremendous investments for cellular infrastructures. Because of the high cost and lack of radio resources, a precise and productive HetNet deployment seems uttermost important. In this work, a flexible four-stage fuzzy logic-based HetNet deployment scheme is proposed, which deploys mix of Macro-eNB, Micro-eNB and relay station (RS) by considering capacity, coverage and cost factors. The proposed scheme identifies the required number of eNBs, their types and deployment locations to offer the expected coverage in a cost-effective way. The simulation results demonstrate that our proposed scheme is more flexible and offers improved performance in terms of system cost and power ratio than the conventional HetNet deployment schemes.

Keywords Coverage ratio · Fuzzy logic · HetNet deployment · MHR · Power ratio · system cost

✉ M. Arthi
arthimdas@gmail.com; arthi.murugadass@vit.ac.in

P. Arulmozhivarman
parulmozhivarman@vit.ac.in

[1] School of Electronics Engineering, VIT University, Vellore Tamil Nadu, India

[2] School of Electrical Engineering, VIT University, Vellore Tamil Nadu, India

1 Introduction

Data traffic has been expanding explosively with the advancement of useful portable terminals, for example, smart phones [1]. The eagerly awaited data tsunami in 2020 time period will require colossal improvements to be experienced by as of now deployed cellular networks [2]. One simple solution to address the above issue is increasing the network capacity. In 2G and 3G networks, network capacity is increased by including additional carriers or cell splitting [3,4]. This arrangement is additionally perplexing and iterative. This will increase the system cost, power consumption and interference. Present wireless standards like LTE and long-term evolution advanced (LTE-A) are well known for lower latency, higher spectral efficiency and flat IP-based architectures [4,5]. 3GPP has been taking a shot at different aspects like carrier aggregation, massive multi-input multi-output (MIMO) and HetNets to further enhance the performance of LTE and LTE-A standards. Spectral efficiency per link performance is drawing closer to the theoretical limits with 3G and 4G standards. The main objective of the future wireless standards is to improve the spectral efficiency per unit area. In other words, the future standards are expected to offer uniform high-quality experience to all the users anywhere inside the cell range.

The only possibility to improve the spectral efficiency per unit area is to increase the node deployment density. This strategy brings the user equipments (UE) closer to the network [3]. This is not possible with the existing Macro-eNBs.

Table 1 Comparison between different LTE eNBs [5]

Parameters	Macro-eNB	Micro-eNB	Pico-eNB	RS
Transmission power	20–40 W	2–20 W	250 mW–2 W	2–20 W
Cell size	≥3 km	250 m–1 km	100 m–300 m	1.125 km [6,7]
Bandwidth	100 MHz	100 MHz	30 MHz	50 MHz
Cost (euros)	397,800	42,200	12,400	55,692 [8]
Users supported	>256	32–200	32–64	>Pico-eNB

Site acquisition with towers in a dense urban territory is troublesome and costly. In 4G standards, the concept of HetNet is very popular, where the conventional high-power Macro-eNB and the low-power Micro-eNB, Pico-eNB, Femto-eNB and RSs are deployed together to offer the service. Different eNBs used in LTE HetNet are compared in Table 1.

Small cells are deployed along with the Macro-eNB to support the UEs in the coverage holes and hotspots [5]. The process of small cells incorporation is required to bolster uneven traffic demand of UEs in a particular area. The Macro-eNB deployment locations should be carefully chosen by network planning with the objectives of achieving maximized coverage and minimized interference between the eNBs [4]. Imperfect network planning leads to severe quality loss. The deployment of small cells is more or less ad hoc. This just requires a rough knowledge of traffic density and coverage holes. The smaller physical size and lower transmit power requirement features make flexible site acquisitions [4,9]. These small cells do not require cooling units to support power amplifiers. Interference mitigation, capacity maximization, site acquisition and infrastructure cost minimization are some of the issues to be addressed by the operators during the network planning [10]. Small cells are boon for the operators, which address the above issues. At whatever point there is an immense traffic demand, Macro-eNB endures by link overloading because of inadequacy of resources. Amid this circumstance, Macro-eNB can off load the data traffic to small cells [5].

Unfortunately, the deployment mechanism of eNBs is not mentioned in any of the standards [7]. Poor deployment schemes cause wasteful spectrum utilization [10]. This likewise prompts serious quality debasement even with the perfect frequency assignment algorithms. There exists a great deal of difficulties connected with HetNet deployment. The deployment ought to address issues like bandwidth, power constraints, link overloading, inter-cell interference and inter-RS interference. A more adaptable and financially savvy cell planning is required by the network operator to offer uniform broadband experience to all UEs in a universal and cost-effective manner.

In 2G standards, cell planning is based on the path loss and signal strength predictions [11]. They do not consider traffic distributions, signal quality necessities and power control [12]. This type of cell planning is not suited for 3G standards. A Tabu search scheme-based mathematical programming model is proposed in [11] for supporting choices on where to deploy new eNBs. The proposed scheme additionally chooses the designs like height of the antenna, tilt, sector orientations, maximum power emission and pilot signal locations. This cell planning is more suited for universal mobile telecommunications system (UMTS) and code division multiple access (CDMA)-2000. It has been proved that the proposed scheme is efficient with reasonable computational time.

A discrete optimization model for UMTS is proposed in [12] for new eNB deployment. This model is based on non-polynomial (NP)-hard. Here, two distinctive randomized greedy algorithms and Tabu search algorithm are utilized for efficient eNB deployment. A cell planning scheme with the goals of coverage and capacity maximization is proposed in [13]. This proposed model is more suited for CDMA-based standards. Here, the cell planning problem is formulated as an integer linear programming model and solved by Tabu search algorithm. The results prove that the proposed scheme outperformed the conventional parallel genetic algorithm-based deployments.

A genetic algorithm-based multi-objective HetNet transmitter deployment scheme is proposed in [14]. The algorithm is meant to fulfill four objectives like coverage expansion, cost minimization, capacity maximization and overlapping index minimization. The algorithm first decides the number of transmitters required to fulfill the above objectives and afterward chooses the heterogeneity of the network. It is proved that the proposed scheme outperforms many conventional single-objective HetNet transmitter deployment schemes.

Macro cell deployment (MCD) scheme deploys only Macro-eNBs like 2G and 3G standards [5]. To offer high-quality services to cell edge UEs, Macro-eNB needs to expand the transmit power level. This prompts larger power consumption. To bolster the uncovered UEs, this scheme always goes for Macro-eNBs irrespective of the number of UEs. This increases the system cost and interference between Macro-eNBs.

Agglomerative hierarchical clustering (AHC) two-type cell deployment (ATD) scheme is discussed in [5,15]. This scheme utilizes modified AHC (MAHC) to frame Macro- and Micro-eNB clusters. After the range adjustment, to bolster

the uncovered UEs, additional Micro-eNBs are deployed. Traditional K-means algorithm proposed in [16] again utilizes MAHC to form Macro- and Micro-eNB clusters. This scheme additionally utilizes K-means algorithm to bolster eNB deployment. The other difference is TKD scheme uses Pico-eNBs to bolster uncovered UEs located far from deployed Macro- or Micro-eNBs. It is likewise demonstrated that these schemes are cost- and power-effective than MCD scheme. In all the above schemes, deployment of RS is not considered.

LTE-A Rel-10 and IEEE 802.16 j standards have presented the idea of MHR systems, where the RSs are utilized to enhance the system performance alongside the eNBs [17,18]. RS deployment is exceptionally helpful in the areas where the eNB backhaul solutions (fibers, microwave links and so on) are unavailable and extremely costly [19]. RSs can likewise be deployed in the territories, where site obtaining for eNB deployment is exceptionally troublesome. Since the deployment and evacuation can be done quicker than the eNB, RSs are best for transitory deployments than eNB. Deployment of RSs in the coverage gaps will enhance the received signal quality of encompassing UEs. This thusly expands the aggregate system capacity without much expanding the capital and operational costs of the operator. The complexity and the cost of the RSs are comparatively much lesser than the eNB. As a result of the more useful nature and less power utilization, RSs will probably be conveyed in the geographic areas than the eNBs. In any case, there exist some significant issues like site and RS selection in MHR systems [17,18]. Until these issues tended to, MHR systems may not fulfill the client requests in terms of throughput and expense. The unsatisfied client will move to the contending operator.

Improper eNB and RS deployment prompts an extreme misfortune in system throughput which thus decreases the throughput per client [20]. Deploying RSs in well-covered regions is likewise inane. The capacity of MHR network is significantly diminished due its two hop transmission [17,18]. Inappropriate RS locations might expand the distance between the communicating nodes. This builds the propagation and information transmission delay, which is an extreme quality issue in time limited real-time applications. Deploying more number of RSs may expand the aggregate deployment cost [19,20]. This thusly builds the average cost per bit. Since the RSs use the same spectrum for the downlink transmission, deployment of more number of RSs will introduce serious inter-RS interference. The inter-RS interference will lessen the signal-to-interference-plus-noise ratio (SINR), which also makes the network to select lower burst profiles during scheduling. More number of RS placements will likewise introduce a path selection issue, which will have a significant impact on the system throughput and transmission delays [21].

Lu and Liao [22] presented a Joint base station (BS) and RS deployment plan (JBRP) for IEEE 802.16 j worldwide interoperability for microwave access (Wi-Max) networks. The problem is modeled with integer linear programming. The recommended scheme boosts the system capacity by guaranteeing the aggregate deployment cost within the limits of maximum permitted deployment budget. This scheme is proposed for a large geographic region with non-uniform traffic demand. Despite the fact that JBRP scheme addressed the coverage and budget constraints, it experiences blemished load distributions between the eNBs. This will prompt in larger packet queuing delay and misfortune in throughput. This is a serious issue regarding client perspective. The unsatisfied client will move to the competing operator. It is likewise assumed that the candidate positions of RSs are same as the locations of UEs and the candidate positions of eNBs are assumed to be the edge of UEs. This is an illogical and preposterous suspicion.

Chang and Lin [7] presented a novel eNB and RS deployment scheme in view of uniform clustering concepts. The proposed scheme uses the modified variant of the K-means algorithm. The algorithm works in two stages, specifically eNB-RS selection stage and eNB-RS deployment stage. This scheme provides sensible throughput and coverage by adjusting the system throughput between distinctive eNBs. There are no exceptional contemplations in the present work for enhancing the system throughput. Chang and Lin [23] introduced a novel eNB and RS deployment scheme in perspective of fuzzy logic. This scheme utilizes fuzzy logic for eNB deployment and deployment factor (DF) for RS deployment. Coverage ratio (CR) and traffic ratio (TR) of each candidate site are given as the input for fuzzy inference engine. The simulation results proved that fuzzy-based scheme requires less number of RSs than the uniform clustering scheme to satisfy the expected coverage and budget constraints. This lessens the system cost. The other important factor is most of the above schemes are tested with free space propagation model, which is unrealistic under practical conditions.

Despite the fact that the aforementioned schemes offer better performance, they do not use the full advantages of LTE HetNet as they deploy just Macro-eNB and RS. Wang and Chuang [5] proposed a novel HetNet deployment scheme for 4G LTE networks. The proposed algorithm involves four stages, where the blend of Macro-eNB, Micro-eNB and Pico-eNB is deployed in the given geographic area to meet the expected coverage and traffic demands. In the first stage, MAHC scheme is utilized to estimate the required number of Macro- and Micro-eNBs to meet the expected coverage. In the second stage, these large cells are deployed in the identified sites from the available candidate sites. In the third stage, each deployed eNB is checked for the availability of band-

width and power resources. Range adjustment is likewise done in this stage, due to which some of the Macro-eNBs are made to Micro-eNBs by shrinking the transmitted power levels. In the last stage, Pico-eNBs are deployed using modified geometric disk cover (MGDC) scheme to bolster the uncovered UEs [24]. It is proved that the given scheme offers enhanced power consumption and reduced system cost over MCD, ATD and TKD schemes. This scheme employs log-distance path loss model specified in LTE Rel-8 to estimate the path loss.

There exist a few disadvantages for the aforementioned scheme. This algorithm utilizes weighted K-means approach to support MAHC scheme in recognizing the quantity of Macro- and Micro-eNBs to bolster the expected coverage and traffic demands. However, K-means approach needs the knowledge of K values ahead of time [5]. This K-means approach does exclude the elements like size of Macro- and Micro-eNBs. The MAHC scheme utilized is complex and iterative. The MGDC scheme used to deploy Pico-eNBs is designed in a manner that only two uncovered UEs can be accommodated. This requires more number of Pico-eNBs, if there are more uncovered UEs, which increases the system cost.

In this work, we have proposed a four-stage HetNet deployment scheme, which addresses the aforementioned issues. In the first stage, we have utilized fuzzy-based Macro-eNB selection and deployment. According to LTE Rel-8, eNB selection is based on the downlink received signal strength [3]. Due to the larger transmit power, the Macro-eNB can cover more number of UEs. But, it may not have sufficient bandwidth and power resources to serve all UEs. To address this issue, range adjustment and resource availability are checked in the second stage. In the third stage, we have utilized RSs to bolster the UEs in the cell edges and coverage holes. Since RS can cover more UEs than Pico-eNB, less number of RSs is adequate to accomplish the expected coverage and traffic. We again utilize fuzzy logic to deploy the RSs. As said before, the capacity of the RSs is restricted when contrasted with the eNBs. At the point when there exists a non-uniform traffic request from a RS, the issue of link overloading emerges [18]. Wang et al. [21] presented a load-aware spectral efficient routing (LASER)-based RS selection scheme which utilizes link spectral efficiency as a metric. This algorithm is turned out to be better performing under link overloading conditions. Thus, in the proposed work, the authors adopt LASER-based RS selection to address the link overloading issue in the fourth stage.

The rest of the script is arranged in the following way. Section 2 presents the system model and Sect. 3 presents the proposed four-stage HetNet deployment scheme. Section 4 examines the proposed system with simulation results, and Sect. 5 concludes the paper by highlighting the future works.

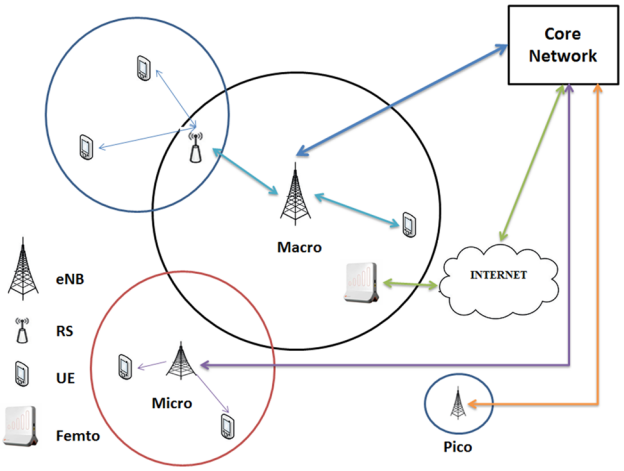

Fig. 1 LTE HetNet with mix of Macro, Micro, Pico, Femto and Relay eNBs

2 System Model

4G wireless networks are typically deployed as HetNet with mix of Macro, Micro, Pico, Femto and Relay eNBs as shown in Fig. 1. This increased serving node density will bring UEs closer to eNB, which increases the network capacity and spectral efficiency per unit area. Pico cells are usually deployed in hotspots, where dependably there exists an immense traffic demand. Whenever there is a shortage of resources, Macro-eNBs usually off load some of the traffic to Pico cells. Pico cells are more suited for outdoor use than Femto cells. Macro, Micro and Pico cells are connected to core network through a wired backhaul connection. The mobile switching center (MSC) acts as a gateway between wired and wireless networks. Femto cells are unplanned network usually deployed by the consumers. It is more suited candidate for high-capacity in-building solutions [25]. It uses consumer's home digital subscriber line (DSL) or cable modem for backhaul connection. The performance of the open Femto cells is similar to the Pico cells [4]. Since this work focuses on the cell planning by the operators, the deployment of Femto cells is not considered here. The idea of MHR network is broadly utilized as a part of LTE-A standard [20]. The RS deployment is more preferable in the areas, where wired backhaul is not available or not sparing. The spectrum used to access the UEs is likewise utilized for backhaul connectivity. RS acts like a UE to Macro-eNB and eNB to serving UEs. Since the deployment of HetNet is not mentioned in any of the standard, it is still an open issue.

2.1 Fuzzy Logic for eNB and RS Deployment

In our proposed system model, we have used the fuzzy approach to identify the optimum deployment locations of

Macro-eNBs and the RSs from the candidate locations. Fuzzy logic controller can include domain knowledge from existing procedures and can be utilized to control complex system [26]. The main advantage of fuzzy concept is that it provides an exact meaning for something, when a precise idea is unavailable and adjusts to a rapid and burst environment.

Chang and Lin [23] proposed a fuzzy logic-based eNB deployment scheme, where the CR and TR of each candidate location are the input for the fuzzy inference system (FIS). They have developed membership functions for CR, TR and selection factor (SF). Based on this, they have developed nine selection rules. Taking into account the coverage requirement and deployment budget, the eNB candidate locations with largest selection factors are chosen for deployment. But, RS deployment is not based on the fuzzy logic. It has been proved that identifying the locations of eNBs using fuzzy technique gives a significant performance improvement when compared with other methods. In the proposed work, we have developed five membership functions for CR, TR and SF. Based upon this, we have framed 25 selection rules. In this work, we select both eNB and RS in light of the fuzzy logic to meet the expected coverage. We have developed membership functions in view of the trapezoidal method, while in the conventional work they have utilized triangular membership functions. We have utilized centroid method for defuzzification [27].

The CR of ith candidate location is the ratio between the number of UEs covered by the eNB (Macro, Micro, Pico or RS) deployed in ith location and the total number of UEs available in the geographic area. It is given by [23]

$$\mathrm{CR}_i = \frac{U_i}{M} \tag{1}$$

where U_i is the number of UEs covered by the eNB deployed in ith location and M is the total number of UEs available in the geographic area.

The TR of ith candidate location is given by

$$\mathrm{TR}_i = \frac{\alpha_{d,i} - \alpha_{t,i}}{\mathrm{Max}\left\{\alpha_{d,i}, \alpha_{t,i}\right\}} \tag{2}$$

where $\alpha_{d,i}$ and $\alpha_{t,i}$ are the average data transmission rate and the average traffic demands of the UEs covered by the eNB deployed in ith location, respectively.

The fuzzy sets for CR of ith candidate location take the linguistic variables like *Very Low, Low, Medium, High, Very High*. These are represented below by the membership functions $\mu^i_{X_1}(\alpha)$, $\mu^i_{X_2}(\alpha)$, $\mu^i_{X_3}(\alpha)$, $\mu^i_{X_4}(\alpha)$ and $\mu^i_{X_5}(\alpha)$, respectively, over the interval [0, 1]:

$$\mu^i_{X_1}(\alpha) = \begin{cases} 1, & \alpha \le 0 \\ \frac{(0.225-\alpha)}{0.225}, & 0 < \alpha < 0.225 \\ 0, & \alpha \ge 0.225 \end{cases} \tag{3}$$

$$\mu^i_{X_2}(\alpha) = \begin{cases} 0, & \alpha \le 0 \\ \frac{\alpha}{0.225}, & 0 < \alpha < 0.225 \\ 1, & 0.225 < \alpha < 0.275 \\ \frac{(0.475-\alpha)}{0.2}, & 0.275 < \alpha < 0.475 \\ 0, & \alpha \ge 0.475 \end{cases} \tag{4}$$

$$\mu^i_{X_3}(\alpha) = \begin{cases} 0, & \alpha \le 0.275 \\ \frac{(\alpha-0.275)}{0.2}, & 0.275 < \alpha < 0.475 \\ 1, & 0.475 < \alpha < 0.525 \\ \frac{(0.725-\alpha)}{0.2}, & 0.525 < \alpha < 0.725 \\ 0, & \alpha \ge 0.725 \end{cases} \tag{5}$$

$$\mu^i_{X_4}(\alpha) = \begin{cases} 0, & \alpha \le 0.525 \\ \frac{(\alpha-0.525)}{0.2}, & 0.525 < \alpha < 0.725 \\ 1, & 0.725 < \alpha < 0.775 \\ \frac{(1-\alpha)}{0.225}, & 0.775 < \alpha < 1 \\ 0, & \alpha \ge 1 \end{cases} \tag{6}$$

$$\mu^i_{X_5}(\alpha) = \begin{cases} 0, & \alpha \le 0.775 \\ \frac{(\alpha-0.775)}{0.225}, & 0.775 < \alpha < 1 \\ 1, & \alpha \ge 1 \end{cases} \tag{7}$$

where $\alpha \in [0,\ 1]$. Figure 2 shows the degree of membership function diagram for CR.

In comparable way, the fuzzy sets for TR of ith candidate location take the linguistic variables like *More Negative, Negative, Center, Positive, More positive*. These are represented below by the membership functions $\mu^i_{Y_1}(\beta)$, $\mu^i_{Y_2}(\beta)$, $\mu^i_{Y_3}(\beta)$, $\mu^i_{Y_4}(\beta)$ and $\mu^i_{Y_5}(\beta)$, respectively, over the interval $[-1, 1]$:

$$\mu^i_{Y_1}(\beta) = \begin{cases} 1, & \beta \le -1 \\ \frac{(-0.55-\beta)}{0.45}, & -1 < \beta < -0.55 \\ 0, & \beta \ge -0.55 \end{cases} \tag{8}$$

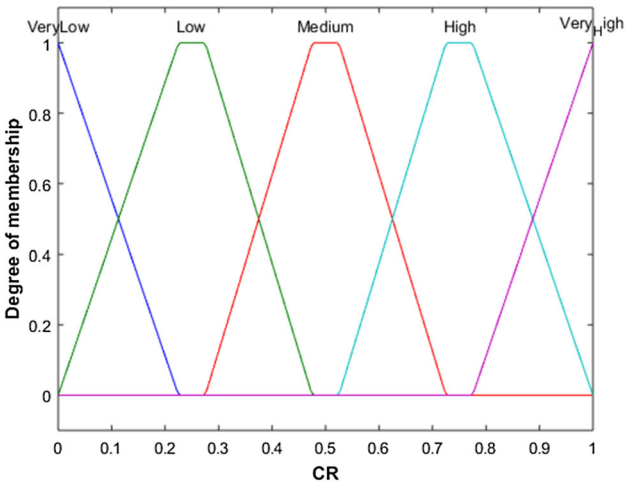

Fig. 2 Degree of membership function diagram for CR

$$\mu^i_{Y_2}(\beta) = \begin{cases} 0, & \beta \le -1 \\ \frac{(\beta+1)}{0.45}, & -1 < \beta < -0.55 \\ 1, & -0.55 < \beta < -0.45 \\ \frac{(-0.05-\beta)}{0.4}, & -0.45 < \beta < -0.05 \\ 0, & \beta \ge -0.05 \end{cases} \quad (9)$$

$$\mu^i_{Y_3}(\beta) = \begin{cases} 0, & \beta \le -0.45 \\ \frac{(\beta+0.45)}{0.4}, & -0.45 < \beta < -0.05 \\ 1, & -0.05 < \beta < 0.05 \\ \frac{(0.45-\beta)}{0.4}, & 0.05 < \beta < 0.45 \\ 0, & \beta \ge 0.45 \end{cases} \quad (10)$$

$$\mu^i_{Y_4}(\beta) = \begin{cases} 0, & \beta \le 0.05 \\ \frac{(\beta-0.05)}{0.4}, & 0.05 < \beta < 0.45 \\ 1, & 0.45 < \beta < 0.55 \\ \frac{(1-\beta)}{0.45}, & 0.55 < \beta < 1 \\ 0, & \beta \ge 1 \end{cases} \quad (11)$$

$$\mu^i_{Y_5}(\beta) = \begin{cases} 0, & \beta \le 0.55 \\ \frac{(\beta-0.55)}{0.45}, & 0.55 < \beta < 1 \\ 1, & \beta \ge 1 \end{cases} \quad (12)$$

where $\beta \in [-1, 1]$. Figure 3 shows the degree of membership function diagram for TR.

The SF of each candidate location is taken as the output parameter from the FIS. The linguistic variables for the SF of ith candidate location are *Very Small, Small, Middle, Large, Very Large*. These are represented below by the membership functions $\mu^i_{Z_1}(\gamma)$, $\mu^i_{Z_2}(\gamma)$, $\mu^i_{Z_3}(\gamma)$, $\mu^i_{Z_4}(\gamma)$ and $\mu^i_{Z_5}(\gamma)$, respectively, over the interval $[-1, 1]$:

$$\mu^i_{Z_1}(\gamma) = \begin{cases} 1, & \gamma \le -1 \\ \frac{(-0.55-\gamma)}{0.45}, & -1 < \gamma < -0.55 \\ 0, & \gamma \ge -0.55 \end{cases} \quad (13)$$

$$\mu^i_{Z_2}(\gamma) = \begin{cases} 0, & \gamma \le -1 \\ \frac{(\gamma+1)}{0.45}, & -1 < \gamma < -0.55 \\ 1, & -0.55 < \gamma < -0.45 \\ \frac{(-0.05-\gamma)}{0.4}, & -0.45 < \gamma < -0.05 \\ 0, & \gamma \ge -0.05 \end{cases} \quad (14)$$

$$\mu^i_{Z_3}(\gamma) = \begin{cases} 0, & \gamma \le -0.45 \\ \frac{(\gamma+0.45)}{0.4}, & -0.45 < \gamma < -0.05 \\ 1, & -0.05 < \gamma < 0.05 \\ \frac{(0.45-\gamma)}{0.4}, & 0.05 < \gamma < 0.45 \\ 0, & \gamma \ge 0.45 \end{cases} \quad (15)$$

$$\mu^i_{Z_4}(\gamma) = \begin{cases} 0, & \gamma \le 0.05 \\ \frac{(\gamma-0.05)}{0.4}, & 0.05 < \gamma < 0.45 \\ 1, & 0.45 < \gamma < 0.55 \\ \frac{(1-\gamma)}{0.45}, & 0.55 < \gamma < 1 \\ 0, & \gamma \ge 1 \end{cases} \quad (16)$$

$$\mu^i_{Z_5}(\gamma) = \begin{cases} 0, & \gamma \le 0.55 \\ \frac{(\gamma-0.55)}{0.45}, & 0.55 < \gamma < 1 \\ 1, & \gamma \ge 1 \end{cases} \quad (17)$$

where $\gamma \in [-1, 1]$. Figure 4 shows the degree of membership function diagram for SF.

The formulated rules for the FIS are described as follows:

Rule 1 If (CR_i is *Very High*) and (TR_i is *More Negative*) then (SF_i is *Middle*)
Rule 2 If (CR_i is *High*) and (TR_i is *More Negative*) then (SF_i is *Middle*)
Rule 3 If (CR_i is *Medium*) and (TR_i is *More Negative*) then (SF_i is *Small*)
Rule 4 If (CR_i is *Low*) and (TR_i is *More Negative*) then (SF_i is *Very Small*)
Rule 5 If (CR_i is *Very Low*) and (TR_i is *More Negative*) then (SF_i is *Very Small*)

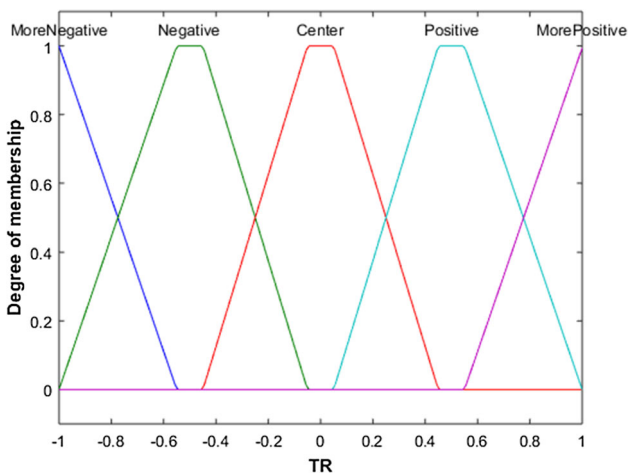

Fig. 3 Degree of membership function diagram for TR

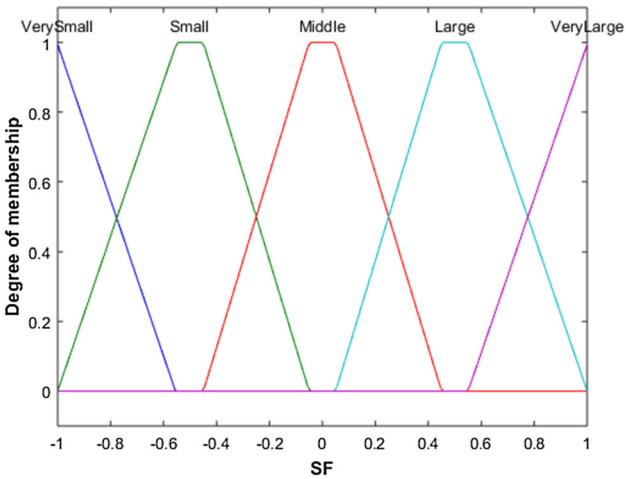

Fig. 4 Degree of membership function diagram for SF

Rule 6 If (CR_i is *Very High*) and (TR_i is *Negative*) then (SF_i is *Large*)
Rule 7 If (CR_i is *High*) and (TR_i is *Negative*) then (SF_i is *Middle*)
Rule 8 If (CR_i is *Medium*) and (TR_i is *Negative*) then (SF_i is *Small*)
Rule 9 If (CR_i is *Low*) and (TR_i is *Negative*) then (SF_i is *Small*)
Rule 10 If (CR_i is *Very Low*) and (TR_i is *Negative*) then (SF_i is *Very Small*)
Rule 11 If (CR_i is *Very High*) and (TR_i is *Center*) then (SF_i is *Very Large*)
Rule 12 If (CR_i is *High*) and (TR_i is *Center*) then (SF_i is *Large*)
Rule 13 If (CR_i is *Medium*) and (TR_i is *Center*) then (SF_i is *Middle*)
Rule 14 If (CR_i is *Low*) and (TR_i is *Center*) then (SF_i is *Small*)
Rule 15 If (CR_i is *Very Low*) and (TR_i is *Center*) then (SF_i is *Very Small*)
Rule 16 If (CR_i is *Very High*) and (TR_i is *Positive*) then (SF_i is *Very Large*)
Rule 17 If (CR_i is *High*) and (TR_i is *Positive*) then (SF_i is *Large*)
Rule 18 If (CR_i is *Medium*) and (TR_i is *Positive*) then (SF_i is *Large*)
Rule 19 If (CR_i is *Low*) and (TR_i is *Positive*) then (SF_i is *Middle*)
Rule 20 If (CR_i is *Very Low*) and (TR_i is *Positive*) then (SF_i is *Small*)
Rule 21 If (CR_i is *Very High*) and (TR_i is *More Positive*) then (SF_i is *Very Large*)
Rule 22 If (CR_i is *High*) and (TR_i is *More Positive*) then (SF_i is *Very Large*)
Rule 23 If (CR_i is *Medium*) and (TR_i is *More Positive*) then (SF_i is *Large*)
Rule 24 If (CR_i is *Low*) and (TR_i is *More Positive*) then (SF_i is *Middle*)
Rule 25 If (CR_i is *Very Low*) and (TR_i is *More Positive*) then (SF_i is *Middle*)

Figure 5 illustrates SF calculation based on CR, TR and If–Then rules.

3 The Proposed HetNet Deployment Scheme

Our proposed algorithm is executed in four stages to meet the following objectives:

$$\frac{1}{M}\left[\sum_{i=1}^{B} b_i U_i + \sum_{j=1}^{R} r_j U_j\right] \geq E_{\mathrm{CR}} \tag{18}$$

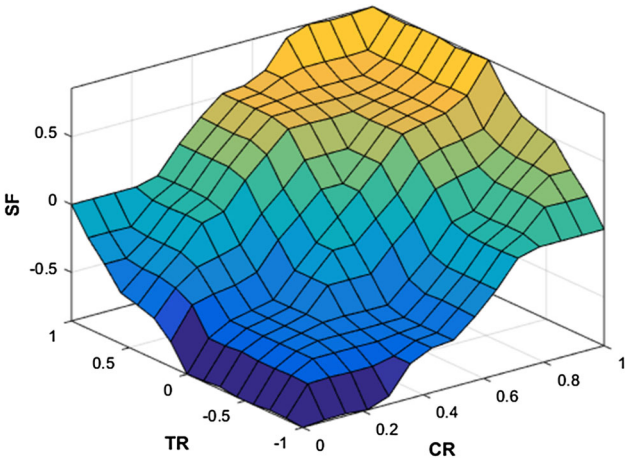

Fig. 5 Surface plot illustrating SF calculation with CR and TR

with the binary function

$$b_i = \begin{cases} 1, & \text{if eNB}_i \text{ is deployed} \\ 0, & \text{else} \end{cases} \tag{19}$$

$$r_j = \begin{cases} 1, & \text{if RS}_j \text{ is deployed} \\ 0, & \text{else} \end{cases} \tag{20}$$

where B and R are the set of candidate locations for eNB and RS deployment, respectively. E_{CR} and Uj are the expected CR and number of UEs covered by jth RS, respectively.

Under the constraints:

1. Power constraint:

$$\sum_{u_m^i \in M} p_{i,m} + \sum_{j=1}^{N^i} p_{i,j} r_{i,j} \leq P_i b_i \tag{21}$$

$$\sum_{u_n^j \in M} p_{j,n}^i \leq P_j r_j; \forall i \in B, j \in R, (m,n) \in M \tag{22}$$

where P_i and P_j are the total transmission power allocated to ith eNB and jth RS, respectively, u_m^i is the mth UE covered by ith eNB and $p_{i,m}$ and $p_{i,j}$ are the transmitted power allocated to mth UE and jth RS by ith eNB, respectively. N^i is the selected candidate locations of RS within the range of ith eNB, u_n^j is the nth UE covered by jth RS and $p_{j,n}^i$ is the transmitted power allocated to nth UE by jth RS in ith eNB.

2. Bandwidth constraint:

$$\sum_{u_m^i \in M} s_{i,m}^{\mathrm{DL}} + \sum_{j=1}^{N^i} s_{i,j}^{\mathrm{DL}} r_{i,j} \leq b_i S_i^{\mathrm{DL}};\ S_i^{\mathrm{DL}} \in \left\{S_{\text{Macro-eNB}}^{\mathrm{DL}}, S_{\text{Micro-eNB}}^{\mathrm{DL}}\right\} \tag{23}$$

$$\sum_{u_n^j \in M} s_{j,n}^{\mathrm{DL}} \leq S_j^{\mathrm{DL}} r_j \tag{24}$$

where S_i^{DL} and S_j^{DL} are the total downlink bandwidth allocated to ith eNB and jth RS, respectively, and $s_{i,m}^{\mathrm{DL}}$ and $s_{i,j}^{\mathrm{DL}}$ are the downlink bandwidth allocated to mth UE and jth RS by ith eNB respectively. $s_{j,n}^{\mathrm{DL}}$is the downlink bandwidth allocated to nth UE by jth RS in ith eNB.

3. $$p_{i,m}, \quad p_{i,j}, \quad p_{j,n}^{i} \geq 0 \tag{25}$$

4. $$s_{i,m}^{\mathrm{DL}}, \quad s_{i,j}^{\mathrm{DL}}, \quad s_{j,n}^{\mathrm{DL}} \geq 0 \tag{26}$$

3.1 Stage 1: Fuzzy-Based Macro-eNB Deployment

The algorithm for fuzzy-based Macro-eNB selection and deployment is illustrated in Fig. 6. The set of candidate locations for Macro-eNB, set of UEs covered by Macro-eNBs and expected CR are given as the input parameters for this algorithm. The identified candidate locations of Macro-eNB are the output from the algorithm. CR and TR of every eNB candidate location are given as the input for FIS, and the relating SF is acquired in steps 2 and 3, respectively. In step 6, candidate location with maximum SF is recognized. In light of this, CR is updated in step 7. If the expected CR is not met, the coordinates of selected candidate location with large SF are stored in **Temp_eNB**. The corresponding SF is made to zero in step 13, so that in step 6, the next maximum SF candidate location will be selected for the next iteration. This process is repeated until the condition in step 8 gets satisfied. All the final identified Macro-eNBs candidate locations with highest SF are stored in **Temp_eNB**.

Stage 1: Selection and deployment of Macro-eNBs

Input: B, u_m, E_{CR}

Output: Temp_eNB=Macro-eNB candidate locations selected for deployment

Initialization: Temp_eNB=Null, CR=0

1. for i=1 to B
2. Calculate CR_i and TR_i using (1) and (2)
3. Identify SF_i using FIS
4. end for
5. for i=1 to B
6. [value index]=max(SF)
7. CR = CR + CR_{index}
8. If CR> E_{CR}
9. break
10. else
11. Temp_eNB = B_{index}
12. end if
13. SF_{index} = 0
14. end for

Fig. 6 Algorithm for Macro-eNB selection and deployment

3.2 Stage 2: Resource Availability Check and Range Adjustment of Macro-eNB

The expected downlink data transmission rate from ith eNB to mth UE is given by [5]

$$r_{i,m}^{\mathrm{DL}} = s_{i,m}^{\mathrm{DL}} \log_2\left(1 + \frac{p_{i,m}^{r} \left|h_{i,m}\right|^2}{s_{i,m}^{\mathrm{DL}} \Gamma \sigma_n^2}\right) \tag{27}$$

where $|h_{i,m}|^2$ is the fading channel gain, σ_n^2 is the noise variance and Γ is the SNR gap. The minimum power requirement of the received signal to achieve the expected downlink rate is given by

$$p_{i,m}^{r} = \left(2^{\frac{r_{i,m}^{\mathrm{DL}}}{s_{i,m}^{\mathrm{DL}}}} - 1\right)\left(\frac{s_{i,m}^{\mathrm{DL}} \Gamma \sigma_n^2}{\left|h_{i,m}\right|^2}\right) \tag{28}$$

The transmitted power from ith eNB to mth UE to support the expected transmission rate is given by

$$p_{i.m}(\mathrm{dB}) = p_{i,m}^{r}(\mathrm{dB}) + \mathrm{PL(dB)};\ \mathrm{PL(dB)} \in \{\mathrm{PL_{Macro}(dB)},\ \mathrm{PL_{Micro}(dB)}\} \tag{29}$$

where $\mathrm{PL_{Macro}(dB)}$ and $\mathrm{PL_{Micro}(dB)}$ are the path loss in dB for Macro and Micro cells which are given by [28,29]

$$\mathrm{PL_{Macro}(dB)} = 128.1 + 37.6 \log_{10}(e) \tag{30}$$

where e is the distance between Macro-eNB and UE or RS.

$$\mathrm{PL_{Micro}(dB)} = 140.7 + 37.6 \log_{10}(e) \tag{31}$$

The concept of resource availability check in eNB is illustrated in Fig. 7. The identified candidate locations of Macro-eNB from the first stage, noise variance, SNR gap, expected data transmission rate, bandwidth allocated per UE, UEs supported by Macro-eNBs, maximum number of UEs an RS can support (V) are given as the input to this algorithm. Identified Macro- and Micro-eNBs for deployment and UEs uncovered by any of the deployed eNBs $\left(\hat{U}\right)$ are the outputs from this algorithm.

The power required to support all UEs covered under ith eNB (p_i) is initialized to 0 in step 2. The distance between mth UE to ith eNB is calculated in step 4. Based on this, path loss and transmit power required to achieve the expected rate

Stage 2: Resource availability check in Macro-eNB

Input: Temp_eNB, $\sigma_n^2, \Gamma, r_{i,m}^{DL}, s_i^{DL}, u_m, v$

Output: Macro and Micro-eNBs selected for deployment, $\hat{U}$

1. for i=1 to length(Temp_eNB)
2. p_i=0
3. for m=1 to U_i
4. $e(m) = |Temp\_eNB(i) - u_m|$
5. Substitute e(m) in (30) to obtain the PL.
6. Calculate $p_{i,m}$ using (29)
7. $p_i = p_i + p_{i,m}$
8. end for
9. If $p_i > P_{Macro\text{-}eNB}$
10. [value index] = max(e)
11. $p_i = p_i - p_{index}$
12. $\hat{U} \leftarrow u_{index}$
13. e(index)=0
14. end if
15. Repeat step 10 to 14 until the (21) gets satisfied
16. Range adjustment (p_i)
17. end for

Fig. 7 Resource availability check in the identified Macro-eNBs

Range adjustment (p_i)

1. If $p_i \le P_{Micro-eNB}$
2. $B_i \rightarrow P_{Micro-eNB}$
3. else if $(U_i - Q_i) \le V$
   where Q_i is the number of UEs getting service from i^{th} Micro-eNB
4. [value index] = max(e)
5. $p_i = p_i - p_{index}$
6. $\hat{U} \leftarrow u_{index}$
7. e(index)=0
8. end if
9. Repeat step 4 to 7, until the (21) gets satisfied

Fig. 8 Concept of range adjustment

are obtained from steps 5 and 6, respectively. The same procedure is repeated for all UEs under ith eNB, and the total power required to support all these UEs is obtained in step 7. If the total power required by ith eNB exceeds $P_{\text{Macro}-\text{eNB}}$, then the farthest UEs are identified and removed from current serving eNB one by one, until the required power constraint is satisfied. This is carried out between steps 9 and 14. The removed UEs are stored in $\hat{U}$, and their corresponding distances are made to zero. This procedure is repeated for all identified Macro-eNBs.

When all the identified Macro-eNBs satisfy the power constraint, the concept of range adjustment is carried out, which is illustrated in Fig. 8. The total power required to support all UEs under each Macro-eNB is compared with the $P_{\text{Micro-eNB}}$ in step 1. When it is true, the power level of the corresponding Macro-eNB is reduced in step 2 so that it acts like a Micro-eNB. Due to this, some of the UEs left uncovered. If the condition given in step 1 is not met, then discard some of the farthest UEs and recheck the condition. Still, if the condition is not met, do not go for range adjustment. The process of removing the farthest UEs should be done only for certain predefined number of UEs, which is taken care in step 3.

Stage 3: Selection and deployment of RSs

Input: CR, R, E_{CR}, $\hat{U}$

Output: Temp_RS=RS candidate locations selected for deployment

Initialization: Temp_RS=Null

1. for j=1 to R
2. Calculate CR_j and TR_j using (1) and (2)
3. Identify SF_j using FIS
4. end for
5. for j=1 to R
6. [value index]=max(SF)
7. $CR = CR + CR_{index}$
8. If $CR > E_{CR}$
9. break
10. else
11. $Temp\_RS = R_{index}$
12. end if
13. $SF_{index} = 0$
14. end for

Fig. 9 Fuzzy-based RS selection and deployment

3.3 Stage 3: RS Deployment to Support Uncovered UEs

The algorithm for fuzzy-based RS selection and deployment is illustrated in Fig. 9. After the completion of second stage, new CR is calculated and that is given as one of the input for RS deployment algorithm. Along with this, set of candidate locations for RS deployment, expected coverage ratio and set of uncovered UEs are also given as the inputs. The identified RS candidate locations are the output from the algorithm. CR and TR of every RS candidate location are given as the input for FIS and the relating SF is acquired in steps 2 and 3, respectively. In step 6, RS candidate location with maximum SF is recognized. In light of this, CR is updated in step 7. If the expected CR is not met, the coordinates of selected candidate location with large SF are stored in **Temp_RS**. The corresponding SF is made to zero in step 13, so that in step 6, the next maximum SF candidate location will be selected for the next iteration. This process is repeated until the condition in step 8 gets satisfied. All the final identified RS's candidate locations with highest SF are stored in **Temp_RS**.

Fig. 10 Concept of resource availability check in RS and LASER-based RS selection

Stage 4: Resource availability check for RS and LASER based RS selection

Input: Temp_RS , $\sigma_n^2, \Gamma, r_{j,n}^{DL}, s_j^{DL}, u_n$

Output: RS selected for deployment

1. for j=1 to length(Temp_RS)
2. p_j=0
3. for n=1 to U_j
4. $e(n) = |Temp\_RS(j) - u_n|$
5. PL is obtained by substituting e(n) in [30]
   $PL_{RS}(dB) = 103.8 + 20.9 \log_{10}(e)$ (32)
6. Calculate $p_{j,n}$.
7. $p_j = p_j + p_{j,n}$
8. end for
9. If $p_j > P_{RS}$
10. [value index] = max(e)
11. $p_j = p_j - p_{index}$
12. Assign u_{index} to the nearby RS, such that the corresponding RS $\in$ Temp_RS based on the availability of the resource.
13. e(index)=0
14. end if
15. Repeat step 9 to 14 until the (22) gets satisfied
16. end for

3.4 Stage 4: Resource Availability Check for RS and RS Selection Based on LASER Scheme

The concept of resource availability check in RS and LASER-based RS selection are illustrated in Fig. 10. The identified candidate locations of RSs from the third stage, noise variance, SNR gap, expected data transmission rate ($r_{j,n}^{\mathrm{DL}}$), bandwidth allocated per UE, UEs supported by RSs are given as the input to this algorithm. Identified RSs for deployment are the output from this algorithm. The power required to support all UEs covered under jth RS (p_j) is initialized to 0 in step 2. U_j mentioned in step 3 represents the number of UEs covered by jth RS. The distance between nth UE to jth RS is calculated in step 4. Based on this, path loss and transmit power required to achieve the expected rate are obtained in steps 5 and 6, respectively. In step 6, transmit power required to support the desired data rate of an UE can be obtained by using the equations similar to (27)–(29). The same procedure is repeated for all UEs under jth RS, and the total power required to support all these UEs is obtained in step 7. If the total power required by jth RS exceeds P_{RS}, then the farthest UEs are identified and removed from current serving RS one by one. This process is repeated until the required power constraint is satisfied. This procedure is repeated for all identified RSs. When all the identified RSs satisfy the power constraint, the concept of LASER-based RS selection is carried out for the UEs which are discarded by serving RSs [21]. The UEs removed from the current serving RS are given service by the neighboring RSs based on the availability of the resource.

The complexity analysis of the proposed algorithm is illustrated here. In first stage, CR and TR are given as the input for FIS. CR computation needs 1 multiplication. TR computation needs 1 addition, 1 multiplication and 1 comparison. To compute SF, FIS uses center of gravity method [23,27], which is given by

$$\mathrm{SF} = \frac{\int \mu_Z(\gamma) \cdot \gamma \, \mathrm{d}\gamma}{\int \mu_Z(\gamma) \, \mathrm{d}\gamma} = \frac{\sum_{i=1}^{p} \mu_Z(\gamma_i) \cdot \gamma_i}{\sum_{i=1}^{p} \mu_Z(\gamma_i)} \tag{33}$$

where p is the number of samples taken to compute SF.

SF computation in step 3 needs **2(p−1)** additions and **(p+1)** multiplications. Steps 1–4 are repeated for B candidate locations of eNB. In step 6, maximum SF is identified which needs **B(B logB)** comparisons. In step 7, CR is updated which needs 1 addition. Steps 5–14 are iterated for B candidate locations of eNB. Thus, the total number of multiplications, additions and comparisons required to execute stage 1 is **B(p+3)**, **2pB** and **B(2+BlogB)**, respectively.

In stage 2, distance between every eNB to all the UEs covered under ith eNB is calculated in step 4. This operation needs 3 multiplications, 5 additions and 2 LUT access. The PL calculation in step 5 requires 1 addition, 1 multiplication and 1 LUT access. $p_{i,m}$ calculation in step 6 requires 1 addition, 1 multiplication and 1 LUT access.

p_i update in step 7 requires 1 addition. All these steps are repeated for U_i number of times. Step 9 requires 1 comparison. In step 10, farthest UEs are identified which requires $\mathbf{U_i logU_i}$ comparisons. p_i update in step 11 requires 1 addition. Steps 9 to 14 are iterated for L number of times. Similarly, range adjustment carried out in step 16 requires $(\mathbf{VU_i logU_i + 2})$ comparisons and $\mathbf{(V+1)}$ additions. The entire process in stage 2 is iterated for **Temp_eNB** number of times. Thus, the total number of multiplications, additions, comparisons and LUT access required to execute stage 2 is $\mathbf{Temp\_eNB} * \mathbf{5U_i}$, $\mathbf{Temp\_eNB} * (\mathbf{8U_i + L + V + 1})$, $\mathbf{Temp\_eNB} * (\mathbf{L(U_i logU_i + 1)} + (\mathbf{VU_i logU_i + 2}))$ and $\mathbf{Temp\_eNB} * \mathbf{4U_i}$, respectively. The computation of stages 3 and 4 is almost similar to stages 1 and 2, respectively. The number of additions, multiplications, comparisons, accesses to LUT for every stage of the proposed algorithm is listed in Table 2.

The complexity comparison of the proposed scheme with the other conventional placement schemes is listed in Table 3. In Table 3, k is the number of clusters, N_u is the number of uncovered UEs, and T is the number of iterations required to calculate final mean point (MP). In Table 3, it is clear that the complexity of the uniform clustering scheme is larger than the fuzzy-based HetNet deployment scheme. The conventional four-stage MAHC-based HetNet placement scheme utilizes MAHC, weighted K-means and MGDC approaches, which are more complex and iterative. This increases the overall computational complexity. Our proposed scheme utilizes fuzzy logic-based eNB and RS placement. Most of the fuzzy operations are logical (except defuzzification). This reduces the overall computational complexity. Even though the fuzzy-based HetNet deployment scheme [23] looks less complex than our proposed scheme, it lags in the system cost, power ratio and total power requirement performances.

4 Simulation Results and Discussion

In this work, MATLAB 2015a-based link level and system level simulations are carried out to validate the performance of the proposed four-stage HetNet deployment scheme. We have also used Vienna LTE system level (v1.8 r1375) and

Table 2 Stage wise complexity analysis of the proposed scheme

Stage	Number of additions	Number of multiplications	Number of comparisons	Number of accesses to look up tables (LUT)
1	2pB	B(p+3)	B(2+BlogB)	–
2	**Temp_eNB**$*(8U_i+L+V+1)$	**Temp_eNB**$*5U_i$	**Temp_eNB**$*(L(U_i \log U_i + 1) + (VU_i \log U_i + 2))$	**Temp_eNB**$*4U_i$
3	2pR	R(p+3)	R(2+RlogR)	–
4	**Temp_RS** $*(8U_j + 2q)$	**Temp_RS**$*5U_j$	**Temp_RS**$*q(U_j \log U_j + 2)$	**Temp_RS**$*4U_j$

Table 3 Complexity comparison of the proposed scheme versus conventional schemes

Schemes	Number of additions	Number of multiplications	Number of comparisons	Number of accesses to LUT
Uniform clustering [7]	13M−2+4k+kT(M−1)+5kB +BR(N_u−1) +BR(B+R−1)+(B+R) +2(B+R)(M−1)+B(k−1) +B(B+R−1)+5R	8k+kT+3kB+3BR +BR(B+R)+2(B+R) +B(B+R) +19M+14R+2	k(B log B) +BR(R log R)+BR +2B+R	5M+2k+2kB+3R
Fuzzy [23]	B(2p−1)+BR(N_u−1) +BR(B+R−1)+2R(M−1) +6R+(B−1) +B(B+R−1)+6M	B(p+3)+3BR +BR(B+R) +B(B+R)+16R +16M+1	2B+BR(R log R+1)	3(M+R)
Four-stage MAHC [5]	7M+4k+kT(M−1) +**Temp_eNB**$*(8U_i+L+V+1)$ +**Temp_pico**$*(8U_j+q)$	3M+8k+kT+7 +**Temp_eNB**$*5U_i$ +**Temp_pico**$*5U_j$	M(M−1)+**Temp_eNB**$*$ $(L(U_i \log U_i+1)+ (VU_i \log U_i+2))$ +**Temp_pico**$*q$ $(U_j \log U_j+1)$	2M+2k +**Temp_eNB**$*4U_i$ +**Temp_pico**$*4U_j$
Proposed	2pB+**Temp_eNB**$*(8U_i+L+V+1)$ +2pR +**Temp_RS**$*(8U_j+2q)$	B(p+3)+**Temp_eNB**$*5U_i$ +R(p+3)+**Temp_RS**$*5U_j$	B(2+B log B)+**Temp_eNB**$*$ $(L(U_i \log U_i+1)$ $+(VU_j \log U_j+2))$ +R(2+RlogR) +**Temp_RS**$*q(U_j \log U_j+2)$	**Temp_eNB**$*4U_i$ +**Temp_RS**$*4U_j$

Table 4 Simulation parameters for configurations

General parameters	
Frequency	2.14 GHz [32]
Bandwidth	Macro-eNB:100 MHz Micro-eNB:100 MHz Pico-eNB:30 MHz RS:50 MHz
Transmission mode	Single antenna
Cost	Macro-eNB:32 units Micro-eNB:3.5 units Pico-eNB:1 unit RS:4.5 units
Traffic model	Full buffer traffic model [33]
Network layout and macroscopic path loss parameters	
Network geometry	Square geographic area with size 10 km × 10 km
Network elements	Macro-eNB, Micro-eNB, Pico-eNB, RS and UE
eNB transmission power	Macro-eNB:40 W Micro-eNB:2 W Pico-eNB:0.25 W RS:4 W
Macroscopic path loss model	Distance-dependent path loss (TS 25.814) [28,29]
Small scale fading	Jakes Rayleigh fading channel [5,34], slow fading
Shadowing	Log normal shadowing [34]
shadowing factor	Macro-eNB:10 dB Micro-eNB:6 dB Pico-eNB:6 dB RS:6 dB
UE settings	
Spatial distribution of UEs	Uniform and non-homogeneous Poisson process [6]
Speed of UE movement	5 kmph
Receiver noise figure	9 dB
Additive white Gaussian noise (AWGN) variance	−174 dBm/Hz
Number of UEs	100–400
Downlink traffic demand of each UE	0.1–1 Mbps
eNB settings	
Antenna gain pattern	Omnidirectional
Inter Macro-eNB distance	500 m
Other parameters	
Target probability of bit error	10^{-6}
SNR gap	7.63
Minimum expected coverage ratio	90 %

link level (v1.3 r1924) simulators, which can be easily integrated with the MATLAB tool [31]. The source codes of these simulators are accessible under non-commercial academic use license. These open source simulators empower reproducible research in the area of wireless communications and comparison of conventional novel algorithms. There exist many commercial simulation tools like Riverbed SteelCentral Modeler, OMNeTCC, ITCC, ns-2,ns-3, GNS3, openWNS and Hurricane II especially designed for LTE-A [32]. The major disadvantages of these simulators are lack in details and accuracy. These simulators leave most of the implementation work to the users. The parameters considered for the simulation study are listed in Table 4.

Assumptions

- The candidate locations for eNB and RS deployment are randomly chosen within the geographic area.
- The deployed RSs are assumed to be fixed RSs. The deployment of nomadic and mobile RSs is not considered in this work.
- The system model is tested only for downlink traffic demands.

There exist various possible solutions to meet the increasing traffic demands and to fulfill the customer expectations for mobile broadband services [35]. One of the solutions is improving the Macro layer capacity with the techniques like more spectrum allocation, massive MIMO and advanced signal processing. These solutions will improve the link spectral efficiency. As indicated in Introduction section, the solutions to improve the link spectral efficiency have already met the fundamental theoretical limits. Thus, this will not help in meeting the mobile broadband objectives. The other solution is densifying the macro layer. Increasing the Macro-eNB density will also increase the system cost, power requirement

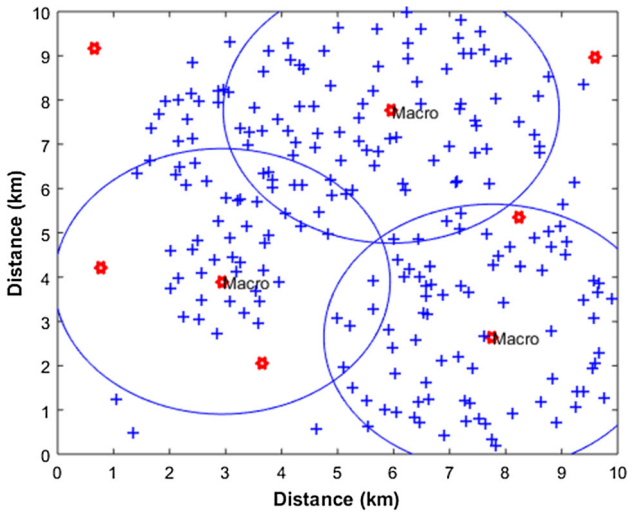

Fig. 11 Sample simulation scenario for stage 1

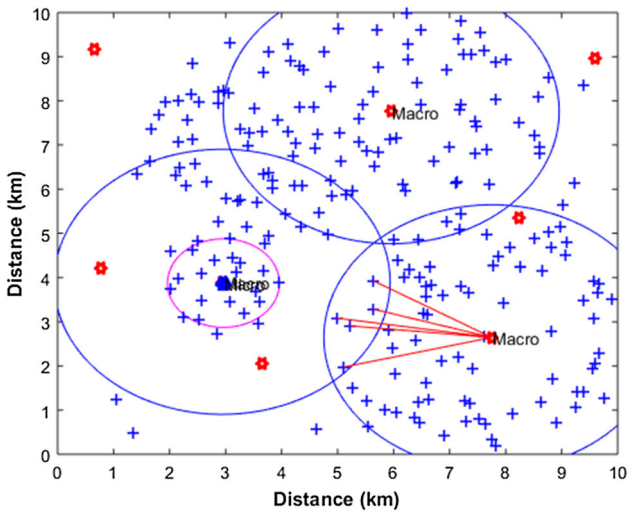

Fig. 12 Sample simulation scenario for stage 2

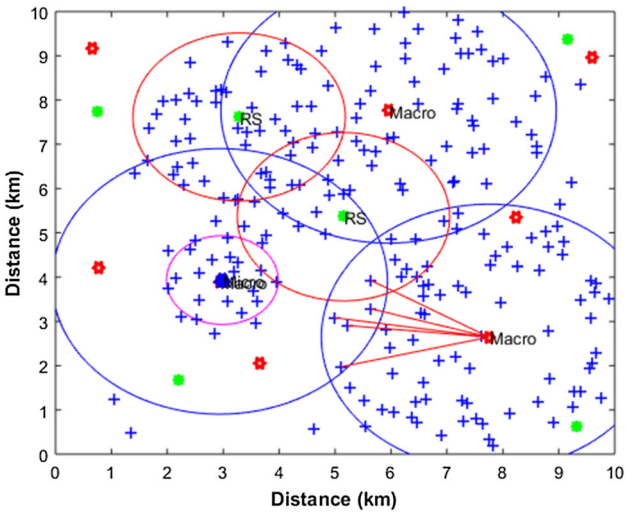

Fig. 13 Sample simulation scenario for stage 3

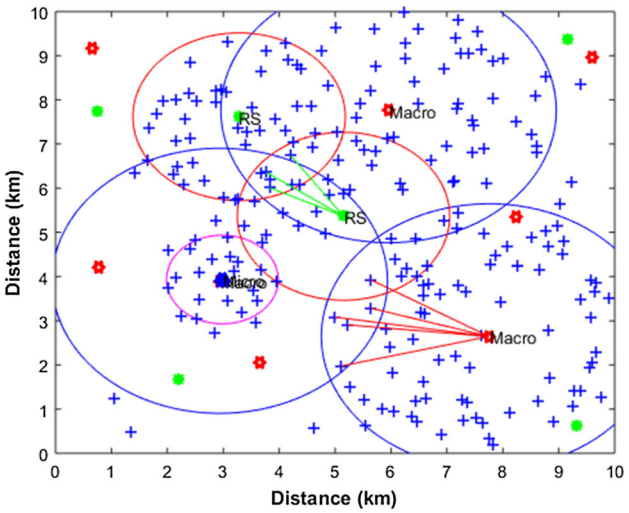

Fig. 14 Sample simulation scenario for stage 4

and inter-cell interference. The site acquisition for Macro-eNB deployment is also a severe issue. Small cell HetNet placement is the simple, low complex solution to meet the expected mobile broadband services. This solution complements Macro layer with low-power nodes. These small cells are usually deployed in the coverage holes, cell edges and hotspots to maximize the coverage. Hence, the CR improvement is considered as one of the outcomes of the proposed algorithm. The minimum expected CR is set to be 90 %. This indicates that at least 90 % of the users should be connected to Macro cells or any small cells or both. The site acquisition, installation and maintenance cost of Macro-eNB are much larger than small cell eNBs. Reducing the system cost is one of the major objectives of the introduction of small cells. Hence, we use system cost as one of the performance metric. Small cells will reduce the distance between the communicating nodes. This reduces the transmission power requirement to meet the expected rate. Hence, total transmission power required by all eNBs is used as another performance metric. In the hotspots and cell edges, Macro-eNB has to effectively offload the portion of the traffic demand to small cells. Power ratio is another metric which measures the effective usage of small cells. A novel HetNet placement scheme should have lower system cost, lower total transmission power and higher power ratio for small cells. Hence, in the proposed work, we use system cost, total transmission power required by all eNBs and power ratio as the performance metrics to validate the performance.

The simulation is repeated for 100 different UE distributions and the average value of system cost, total power requirement and power ratio are displayed in this work. Some of the sample simulation scenarios of the proposed scheme are shown in Figs. 11, 12, 13 and 14, respectively. During the first stage of deployment, 3 Macro-eNBs sites are selected out of 8 candidate locations based on the fuzzy logic. This

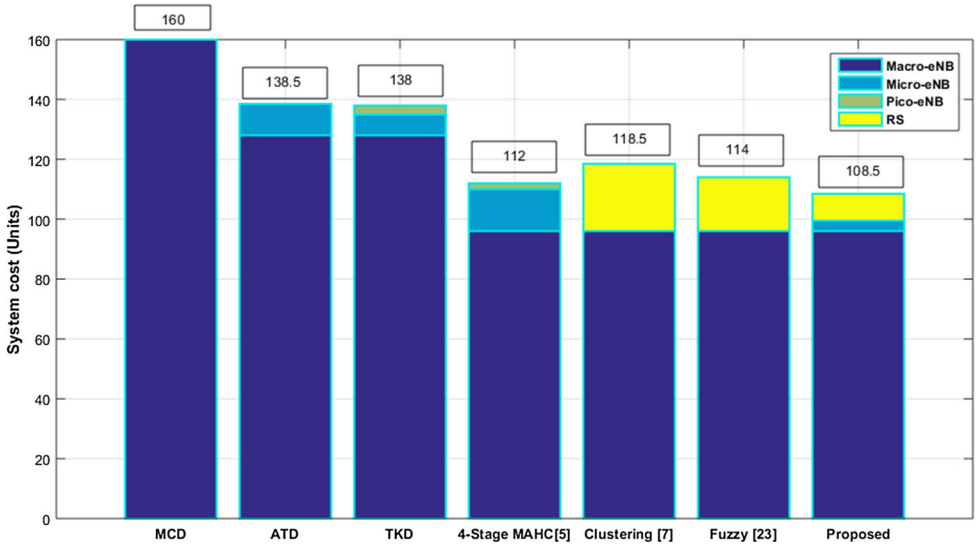

Fig. 15 System cost comparison for different HetNet deployment schemes

is shown in Fig. 11. In second stage, resource availability check and range adjustments are carried out, which is displayed in Fig. 12. After resource availability check and range adjustment, one of the deployed Macro-eNBs transmit power level is reduced so that it acts like a Micro-eNB. Due to this range adjustment, some of the UEs become uncovered by the current eNB. Based on the availability of the resources, the services of these UEs are handed over to neighboring eNBs. This is shown in Fig. 12, where some of the UEs in overlapping area are handed over to next Macro-eNB. This is highlighted with red color lines. The UEs uncovered by any of these eNBs are supported by RSs. Some of the UEs may be covered by neighboring eNBs, but the eNBs may not have sufficient resources to serve them. These UEs are also served by RSs. In stage 3, RSs are selected from the candidate locations based on the fuzzy logic. The selected RSs are used for coverage extension. The scenario corresponding to stage 3 is shown in Fig. 13. Again, the capacity of the RS is limited when compared with Macro-eNB. Insufficient resources may lead to link overloading problems in RSs. In stage 4, some of the UEs in the overlapping RS areas are handed over to the neighboring RS based on the availability of the resources. This ensures increased throughput per user and reduces the delay. This is illustrated in Fig. 14.

Figure 15 compares the total system cost required by various HetNet deployment schemes. It is observed that the system cost increases with the number of UEs, irrespective of the deployment schemes. Since the MCD scheme always considers Macro-eNBs, the system cost for this scheme is always higher than the other schemes. It is noticed that the system cost for ATD and TKD approaches are almost same. Both of these approaches use MAHC scheme to deploy Macro-eNBs. This results in same number of deployed Macro-eNBs for both of these schemes. Since ATD scheme does not employ Pico-eNBs, it needs slightly more number of Micro-eNBs than TKD. The scheme proposed in [5] utilizes range adjustment-based Micro-eNB deployment and MGDC scheme-based Pico-eNB deployment, which actually reduces the required number of Macro-eNBs. Uniform clustering and fuzzy schemes deploy only Macro-eNBs and RSs. Since RS can cover more number of UEs than Micro-eNB and Pico-eNB, the system cost required by these schemes is lower than the MCD, ATD and TKD schemes. Fuzzy scheme requires less number of RSs than the uniform clustering scheme to offer same coverage [36]. This results in slightly less system cost than uniform clustering scheme. Our proposed scheme optimally deploys Macro-eNB, Micro-eNB and RS based on the traffic demand and UE distributions. The proposed scheme utilizes fuzzy logic for both Macro-eNB and RS deployment. The combination of fuzzy logic and range adjustment minimizes the unwanted deployments, which in turn minimizes the total system cost-effectively. This efficient deployment reduces the system cost approximately by 3 % compared with the conventional scheme in [5].

Figure 16 shows total power requirement by all eNBs (W) versus downlink traffic demand (Mbps) for various HetNet deployment schemes. As mentioned earlier, the downlink traffic demand of each service acquiring UEs is varied between 0.1 and 1 Mbps. To achieve an expected data rate, eNB has to allocate different power levels to each UE based on the path loss and fading channel conditions. Increase in the traffic demand will also increase the transmit power level, which also increases the aggregate power required by all eNBs. In MCD scheme, Macro-eNB uses large transmit power to cover maximum number of UEs. It always deploys Macro-eNBs even to cover small number of uncovered UEs. To offer high data rate to cell edge users, Macro-eNB has to increase the transmit power level. Thus, MCD scheme always consumes more transmit power than the other schemes. ATD scheme uses Micro-eNB to cover uncovered UEs. This will

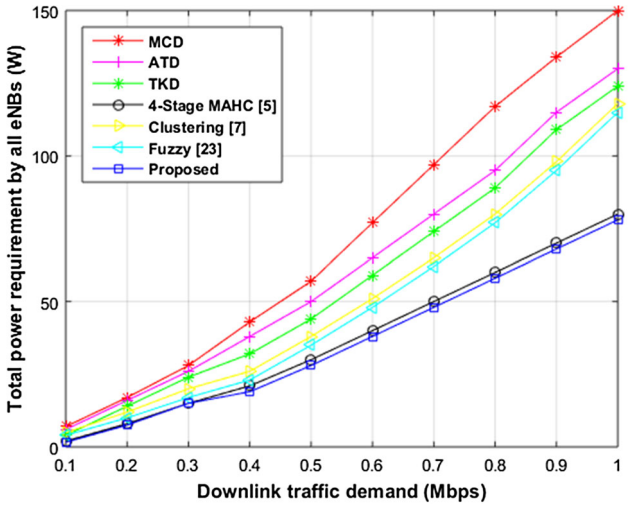

Fig. 16 Total power requirement by all eNBs (W) versus downlink traffic demand (Mbps) for various HetNet deployment schemes

reduce the total power requirement of ATD scheme than MCD scheme. TKD scheme offers better power consumption performance than ATD scheme since it utilizes Pico-eNBs to support uncovered UEs. In uniform clustering and fuzzy-based deployment schemes, the network consists of only Macro-eNBs and RSs. Since RSs can cover more UEs than Pico-eNBs, the total power consumption of these schemes is very less than MCD, ATD and TKD schemes. The scheme proposed in [5] includes range adjustment-based Micro-eNB deployment and MGDC scheme-based Pico-eNB deployment. The idea of shrinking the coverage range and inclusion of Pico-eNBs to support uncovered UEs will reduce the total power consumption. Our proposed scheme deploys mixture of Macro-eNB, Micro-eNB and RS effectively, which makes service offering nodes closer to UEs. This minimizes the total power consumption. The power consumption performance of our proposed scheme is almost similar or even better than the conventional scheme in [5]. From Fig. 16, it is clear that to achieve the expected downlink data rate of 1 Mbps, the total power required by all the deployed eNBs of our proposed scheme is 78 W. From Fig. 14, it is clear that the total power constraint of deployed Macro, Micro and RS is 86 W. Thus, total power required by the proposed scheme is less than the power constraint.

Figure 17 shows power ratio comparison between different HetNet deployment schemes. The power ratio is the measure of ratio of power required by Macro-eNB, Micro-eNB, Pico-eNB and RS to achieve the specific downlink traffic demand. Since MCD scheme deploys only Macro-eNBs, the power consumed by Macro-eNB is 100 %, whereas for other type of eNBs and RS, it is zero. Since ATD and TKD approaches use MAHC, they deploy same number of Macro-eNBs. In these two schemes, almost 96 % of power is consumed by the Macro-eNBs. In ATD scheme, remaining 4 % of power is consumed by Micro-eNB. In TKD scheme, the power consumed by Micro-eNB and Pico-eNB is 2.9 and 1.1 %, respectively. It should be noted that all these methods do not effectively use LTE HetNet. The uniform clustering scheme deploys more number of RSs than the fuzzy scheme to offer the expected coverage. The power consumption of RSs in uniform clustering and fuzzy-based schemes is 19.8 and 18.2 % respectively. The power consumption by small cells of the scheme proposed in [5] and our proposed scheme is 22.2 and 28.4 %. This implicitly indicates that our proposed scheme efficiently utilizes LTE HetNet. Hence, this solution solves the traffic demand and coverage problems of the UEs by efficiently offloading portion of the traffic to small cells and by extending the coverage.

Fig. 17 Power ratio comparison between different HetNet deployment schemes

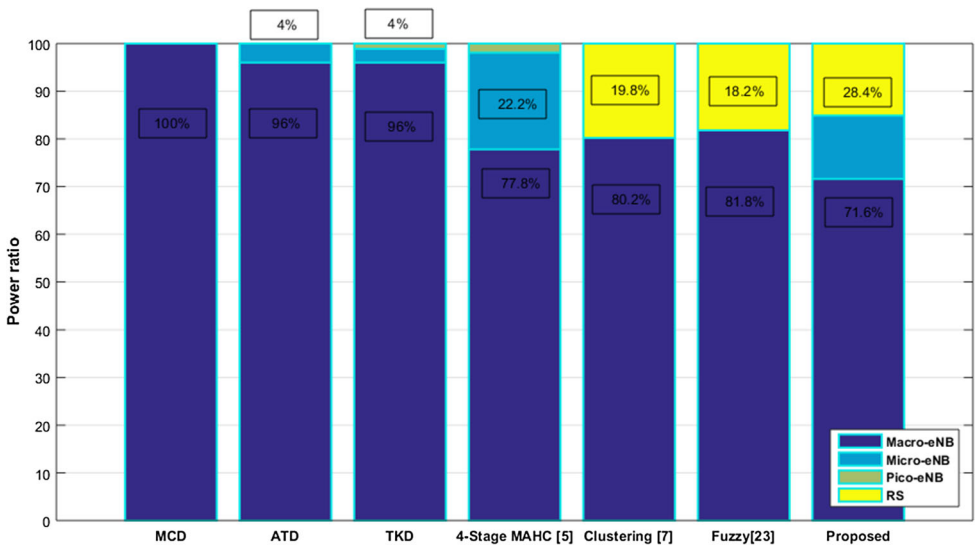

5 Conclusions

A four-stage fuzzy logic-based cost- and power-effective HetNet deployment scheme is proposed in this work. The proposed scheme effectively supports decisions on the number of HetNet nodes, their types and placement locations to meet the expected coverage. The proposed scheme offers an average CR of more than 95 %, which is greater than the expected CR of 90 %. The simulation results prove that our proposed scheme effectively utilizes the HetNet than the other conventional deployment schemes. It effectively off loads portion of the data traffic to small cells in hotspots. In terms of power ratio, our proposed scheme shows an improvement of approximately 6 % over the conventional scheme proposed in [5]. This efficient deployment also reduces the system cost approximately by 3 % compared with the conventional scheme proposed in [5]. Our proposed scheme is also less computationally complex than many of the conventional schemes. The system is tested for a small geographic area. When it is extended for the large geographic area, the gains achieved will also increase. Thus, the proposed scheme effectively finds a trade-off between maximizing the coverage and minimizing the system cost. The present deployment scheme is tested only for coverage constraint. This can also be extended for budget constraint. Similarly, the proposed scheme can also be extended for bandwidth constraint. Already the network providers deployed many Macro-eNBs. Since site acquisition is expensive, it is very difficult to redeploy new Macro-eNBs. The proposed algorithm can be modified in such a way that it can use the existing Macro-eNBs and adds small cells to satisfy the traffic demands of the customers in a cost-effective way.

References

1. Kaneko, S.; Matsunaka, T.; Kishi, Y.: A cell-planning model for HetNet with CRE and TDM-ICIC in LTE-Advanced. In: IEEE Vehicular Technology Conference, pp. 1–5 (2012)
2. Gelabert, X.; Zhou, G.; Legg, P.: Mobility performance and suitability of macro cell power-off in LTE dense small cell HetNets. In: IEEE International Workshop on Computer Aided Modeling and Design of Communication Links and Networks, pp. 99–103 (2013)
3. Khandekar, A.; Bhushan, N.; Tingfang, J.; Vanghi, V.: LTE-advanced: heterogeneous networks. In: European Wireless Conference, pp. 978–982 (2010)
4. Damnjanovic, A.; Montojo, J.; Wei, Y.; Ji, T.; Luo, T.; Vajapeyam, M.; Yoo, T.; Song, O.; Malladi, D.: A survey on 3GPP heterogeneous networks. IEEE Wirel. Commun. **18**(3), 10–21 (2011)
5. Wang, Y.-C.; Chuang, C.-A.: Efficient eNB deployment strategy for heterogeneous cells in 4G LTE systems. Comput. Netw. **79**, 297–312 (2015)
6. Chang, B.J.; Liang, Y.H.; Su, S.S.: Analyses of relay nodes deployment in 4G wireless mobile multihop relay networks. Wirel. Pers. Commun. **83**(2), 1159–1181 (2015)
7. Chang, J.Y.; Lin, Y.S.: A clustering deployment scheme for base stations and relay stations in multi-hop relay networks. Comput. Electr. Eng. **40**(2), 407–420 (2014)
8. Wener, M.; Moberg, P.; Skillermark, P.: Cost assessment of radio access network deployment with relay nodes. In: ICT-Mobile Summit 2008 Conference Proceedings (2008)
9. Barbera, S.; Michaelsen, P.H.; Saily, M.; Pedersen, K.: Mobility performance of LTE co-channel deployment of macro and pico cells. In: IEEE Wireless Communications and Networking Conference, pp. 2863–2868 (2012)
10. Goudos, S.K.; Plets, D.; Liu, N.; Martens, L.; Joseph, W.: A multi-objective approach to indoor wireless heterogeneous networks planning based on biogeography-based optimization. Comput. Netw. **91**, 564–576 (2015)
11. Amaldi, E.; Capone, A.; Malucelli, F.: Radio planning and coverage optimization of 3G cellular networks. Wirel. Netw. **14**(4), 435–447 (2008)
12. Amaldi, E.; Capone, A.; Malucelli, F.: Planning UMTS base station location: optimization models with power control and algorithms. IEEE Trans. Wirel. Commun. **2**(5), 939–952 (2003)
13. Lee, C.Y.; Kang, H.G.: Cell planning with capacity expansion in mobile communications: a Tabu search approach. IEEE Trans. Veh. Technol. **49**(5), 1678–1691 (2000)
14. Ting, C.K.; Lee, C.N.; Chang, H.C.; Wu, J.S.: Wireless heterogeneous transmitter placement using multiobjective variable-length genetic algorithm. IEEE Trans. Syst. Man Cybern. Part B Cybern. **39**(4), 945–958 (2009)
15. Lung, C.H.; Zhou, C.: Using hierarchical agglomerative clustering in wireless sensor networks: an energy-efficient and flexible approach. Ad Hoc Netw. **8**(3), 328–344 (2010)
16. Wu, J.: Advances in K-means Clustering: A Data Mining Thinking. Springer, New York (2012)
17. Arthi, M.; Arulmozhivarman, P.; Babu, K.V.; Reddy, G.R.; Barath, D.: Techniques to enhance the quality of service of multi hop relay networks. Proc. Comput. Sci. **46**, 973–980 (2015)
18. Arthi, M.; Joy, J.J.; Arulmozhivarman, P.; Babu, K.V.: An efficient relay station deployment scheme based on the coverage and budget constraints in multi-hop relay networks. In: IEEE International Conference on Communication and Signal Processing, pp. 122–126 (2015)
19. Akyildiz, I.F.; Gutierrez-Estevez, D.M.; Balakrishnan, R.; Chavarria-Reyes, E.: LTE-advanced and the evolution to beyond 4G (B4G) systems. Phys. Commun. **10**, 31–60 (2014)
20. Arthi, M.; Arulmozhivarman, P.; Babu, K.V.: Quality of service aware multi-hop relay networks for green radio communication. J. Green Eng. **5**, 1–22 (2015)
21. Wang, S.S.; Lien, C.Y.; Liao, W.H.; Shih, K.P.: LASER: a load-aware spectral-efficient routing metric for path selection in IEEE 802.16 j multi-hop relay networks. Comput. Electr. Eng. **38**(4), 953–962 (2012)
22. Lu, H.C.; Liao, W.: Joint base station and relay station placement for IEEE 802.16j networks. In: Proceedings of IEEE Global Telecommunications Conference, (GLOBECOM) (2009)
23. Chang, J.Y.; Lin, Y.S.: An efficient base station and relay station placement scheme for multi-hop relay networks. Wirel. Pers. Commun. **82**(3), 1907–1929 (2015)
24. Wang, Y.C.; Chen, Y.F.; Tseng, Y.C.: Using rotatable and directional (R&D) sensors to achieve temporal coverage of objects and its surveillance application. IEEE Trans. Mob. Comput. **11**(8), 1358–1371 (2012)
25. Fujitsu: High-Capacity Indoor Wireless Solutions: Picocell or Femtocell. http://www.fujitsu.com/downloads/TEL/fnc/whitepapers/High-Capacity-Indoor-Wireless.pdf (2014)
26. Iancu, I.: A Mamdani Type Fuzzy Logic Controller. INTECH Open Access Publisher, Rijeka (2012)

27. Bede, B.: Single input single output fuzzy systems. In: Kacprzyk, J. (ed.) Studies in Fuzziness and Soft Computing, pp. 105–136. Springer, Heidelberg (2013)
28. European Telecommunications Standards Institute: LTE; Evolved Universal Terrestrial Radio Access (E-UTRA); Radio Frequency (RF) system scenarios (3GPP TR 36.942 version 8.2.0 Release 8). Technical Report, ETSI TR 136 942 V8.2.0 (2009-07)
29. European Telecommunications Standards Institute: LTE; Evolved Universal Terrestrial Radio Access (E-UTRA); Radio Frequency (RF) requirements for LTE Pico Node B. Technical Report, ETSI TR 136 931 V9.0.0 (2011)
30. 3GPP TR 36.826 V11.0.0 (2012-09): 3rd Generation Partnership Project; Technical Specification Group Radio Access Network; Evolved Universal Terrestrial Radio Access (E-UTRA); Relay radio transmission and reception (Release 11) (2011)
31. Mehlführer, C.; Ikuno, J.C.; Simko, M.; Schwarz, S.; Wrulich, M.; Rupp, M.: The Vienna LTE simulators-enabling reproducibility in wireless communications research. EURASIP J. Adv. Signal Process. **2011**, 29 (2011)
32. Taranetz, M.; Blazek, T.; Kropfreiter, T.; Muller, M.K.; Schwarz, S.; Rupp, M.: Runtime precoding: enabling multipoint transmission in LTE-advanced system-level simulations. IEEE Access **3**, 725–736 (2015)
33. Martín-Sacristán, D.; Monserrat, J.F.; Osa, V.; Cabrejas, J.: LTE-Advanced System Level Simulation Platform for IMT-Advanced Evaluation. Waves 15–23 (2011). http://www.iteam.upv.es/pdf_articles/42.pdf
34. Cho, Y.S.; Kim, J.; Yang, W.Y.; Kang, C.G.: MIMO-OFDM Wireless Communications with MATLAB. Wiley, New York (2010)
35. Landström, S.; Furuskär, A.; Johansson, K.; Falconetti, L.; Kronestedt, F.: Heterogeneous networks-increasing cellular capacity. The data boom: opportunities and challenges. Ericsson Rev: Commun Technol J. **4**, 4–9 (2011)
36. Mariya, V.; Babu, K.V.; Arthi, M.; Arulmozhivarman, P.: A novel fuzzy based relay node deployment scheme for multi-hop relay network. In: International Conference on Emerging Trends in Engineering, Science and Technology (ICETEST) (2015)